Journal of Engineering and Sustainable Development
www.jeasd.org
Vol. 22, No.03, May 2018
ISSN 2520-0917

THE USE OF TRANSMISSIBILITY FUNCTIONS FOR DAMAGE IDENTIFICATION IN REINFORCED CONCRETE BEAMS

Dr. Ali Abdulhussein Al-Ghalib[1]* Dr. Sawsan Mousa Mahmoud[2]

1) Lecturer, Civil Engineering Department, Mustansiriayh University, Baghdad, Iraq.
2) Lecturer, Computer Engineering Department, Mustansiriayh University, Baghdad, Iraq.

Abstract: Nowadays, structural health monitoring is the area of a great interest of continuing research aiming at establishing a reliable condition monitoring strategy of civil engineering infrastructure. Such finding will allow moving from the schedule-based inspection policy to condition-based policy. This study is dedicated to identify the damage in reinforced concrete beams by using only frequency domain vibration measurements. In the meantime, statistical pattern recognition model was tested through the course of this research. A transmissibility-based damage detection and classification system was proposed. Subsequently, the measure distance of the spectra envelope (COSH) was suggested as classification tool. The proposed method was examined on datasets from numerical beam model and experimental measurements from 2.0m reinforced concrete beam. For the two models, the results of the proposed approach proved effective and managed to detect various levels of defects, and classify the defects according to their size. Having processed response signals to detect and classify state conditions, the devised approach is relevant to use in embedded online structural health monitoring.

Keywords: *Structural health monitoring, transmissibility functions, experimental modal analysis, reinforced concrete beams*.

أستعمال الانتقالية لاشارة الاهتزاز الديناميكية لتحديد الضرر في العتبات الخرسانية

الخلاصة: يعتبرموضوع مراقبة سلامة المنشأت هذه الايام من المواضيع ذات الاهتمام البحثي المتزايد بهدف الوصول الى استرتيجية معتمدة لمراقبة منشأت البنى التحتية. ستتيح هكذااستراتيجية التحول من برامج المراقبة المقررة مسبقا الى برامج للتقييم تبعا للاداء. هذه الدراسة مكرسة لتقييم الضررفي العتبات الخرسانية باستخدام قياسات الاهتزازضمن نطاق الترددات. في نفس الوقت تم اختبار نموذجا احصائيا للتعرف على نوع وشدة النمط. تم استخدام متغيرالأنتقالية كميزة للكشف وتحديد نوع الضرر، اضافة الى ذلك تم استخدام طول الغلاف الطيفي كاداة لتصنيف الضرر.اختبرت الطريقة المقترحة على نماذج نظرية ونموذج حقيقي مختبري لعتبة من الخرسانة المسلحة. اخضعت جميع النماذج لضررمتزايد نتيجة التحميل. تمكن النموذج الاحصائي المقترح من الكشف على الضرر وتحديد مداه وتصنيف الأنواع المختلفة من الضررحسب شدتها.

1. Introduction

Civil engineering infrastructure owners, users, consultants and contractors are of serious anxiety of the limited reliability of the onerous visual inspection and other non-destructive testing (NDT) systems. The increased number of aged and sophisticated structures has clearly made the failure of current NDT tools undeniable. Conversely, researchers over the last four decades have opted for examining and adapting the

*Corresponding Author:ali.alghalib@uomustansiriyah.edu.iq

vibration-based methods to monitoring and assessing of civil infrastructures. Even with the presence of the experimental errors, measurements from these methods give a more reliable representation for a tested structure compared with the simulated analytical model [1]. In spite of the great level of research that the vibration-based monitoring systems witnessed, a vigorous approach of indicating an abnormal condition of a structure has yet to be developed and widely applied [2.[

Modal testing is the most common method in vibration testing techniques. By carrying out the experimental modal analysis (EMA) of a structure, the frequency response function (FRF) can be obtained, and modal parameters, such as resonance frequency, modal damping, mode shapes, and their combinations can be extracted. This will make possible the construction of different damage indicators [3]. Nonetheless, model-based analysis methods that use modal parameters are computationally tedious, lengthy and they are unfeasible to exploit in online real-time monitoring [4]. The human ability to evaluate abundant instantaneous amounts of data is extremely limited; therefore, statistical pattern recognition (SPR) techniques need to be introduced into the business. The procedure scrutinises the incoming data and informs the operator of unusual events [4]. On the whole, the subject of structural health monitoring (SHM) has been studied as SPR application by researchers since the beginning of the last decade. As a replacement or supplement to the model-based methods, a number of researchers from the National Laboratory in Los Alamos have recommended a new approach of four-part paradigm for an effective damage identification; namely operational evaluation, data acquisition and data cleansing, feature extraction and statistical modelling [5, 6].

Modal testing is also conducted on structures in real operational conditions, within which the excitation will be very difficult or even impossible to be measured. Operational modal analysis (OMA) uses the response signals only to extract the structural dynamic parameters in order to assess the structural states. The emerging of the real-time OMA has motivated the subject of SHM paradigm of civil engineering infrastructure. SHM is rather a new model for monitoring of civil infrastructure, where it has been significantly developed in the last two decades in both academic research and applications. This area has witnessed a speeding up of development in the sensing technology, data mining, system identification, and condition assessment [7 .[

In real engineering applications, motivated by solving the difficulty in capturing the excitation, in the middle of 1980s, transmissibility functions (TFs) was raised [3]. Instead of considering the input and output signals of the structural system, transmissibility concentrates only on the outputs. That is, it exploits the interrelation of two outputs of the structure in order to make a connection with the structural dynamic characteristic.

The main part of the acknowledged literature that uses transmissibility functions was being accentuated on concentrated faults [3, 8, 9 and 10]. Therefore, this paper makes a visit to the problem of damage detection and quantification in a reinforced concrete (RC) beam modeled with progressive damage scenario. The study aims at validating the TFs as damage sensitive features in real concrete elements where the nonlinear behavior is significant and faults broaden over distinct length. The advantage of implementing

these features is that they use only responses of the structure and as a result can give identification even if the ambient excitation is unknown [11]. Amid the struggling of damage identification industry in finding a reliable feature for the damage identification using raw dynamic datasets, TF appears as a recognized parameter to do the job.

The structure of this paper is outlined as follows: the following two sections submit a brief description of the relevant approach. Section 4 of the paper discusses a numerical simulation as a case study. In section 5, the suggested approach is tested against experimental measurements of civil engineering interest.

2. Vibration Transmissibility Function

The transmissibility can be defined as the non-dimensional quantity that at each frequency computes how much disturbance has overtaken from the source to the receiver through the transmission path [12].

According to Dynamic Testing Agency (DTA) of UK [13], transmissibility is defined as:

"The non-dimensional ratio of response amplitude of a system in steady state forced vibration to the excitation amplitude. This ratio can be expressed in term of forces, displacements, velocities or accelerations."

Ewins [14] defined the transmissibility of vibration as the ratio between the response levels at two points, say j and k, due to a single excitation, say at degree of freedom (DOF) i. Following these definitions, the transmissibility can be written as:

$$T_{jk}^{i} = \frac{H_{ji}(\omega)}{H_{ki}(\omega)} \qquad (1)$$

Where: $H_{ji}(\omega)$ and $H_{ki}(\omega)$ are FRFs corresponding to the responses at points j and k, respectively, due to an excitation at DOF i, and H represents the FRF.

Based on the above definition, transmissibility can be regarded as a quantity that indicates the ratio of vibration levels between two points on the structure.

FRF relationship for a linear structure in the frequency domain can be expressed as [15]:

$$X(\omega) = H(\omega)F(\omega) \qquad (2)$$

Where: $F(\omega)$ and $X(\omega)$ are the input (force) frequency spectrum and output (response) frequency spectrum, respectively. The sampled digital signals are transferred to the frequency components using Fourier transform (Fourier series) in order to calculate the complex Fourier components of the signals.

Therefore, the transmissibility function between two points will be:

$$T_{jk}^{i} = \frac{X_{ji}(\omega)/F_{i}(\omega)}{X_{ki}(\omega)/F_{i}(\omega)} = \frac{X_{ji}(\omega)}{X_{ki}(\omega)} \qquad (3)$$

However, the direct transmissibility can be estimated using two response signals without passing through the calculations of FRF as:

$$T_{jk}^{i} = \frac{X_{ji}(\omega)}{X_{ki}(\omega)} \cdot \frac{X_{ki}(\omega)}{X_{ki}(\omega)} = \frac{S_{jk}(\omega)}{S_{kk}(\omega)} \qquad (4)$$

Where: S_{kk} and S_{jk} are the auto spectra and cross spectra of the output signals, respectively.

3. Novelty Detection Approach

The detection analysis of the transmissibility function is only a qualitative means of discrimination features for different structural conditions. Thus, there is a necessity to set threshold values for the basic reference measurements that can be exploited to evaluate/compare if statistically significant changes have occurred in the new set the ambiguous measurements. Novelty detection approaches are typically exploited for this purpose. One of the straight and easiest ways to achieve that is to obtain the amount of difference between discrete spectral distances from various transmissibility functions. The adjustment of the symmetrical Itakura-Saito discrete spectral distance defined as COSH distance gives a complete estimate of the difference between two discrete spectral envelopes [16]. Trendafilova and other outstanding researchers have adapted Itakura-Saito spectral distance to use with FRF, whereas the author herein suggests using the same formula for transmissibility function. The new version of the COSH spectral distance can be expressed as:

$$\mathrm{COSH}(T, \overline{T}) = \frac{1}{2n} \sum_{i=1}^{n} \frac{T(\omega_i)}{\overline{T}(\omega_i)} - \log \frac{T(\omega_i)}{\overline{T}(\omega_i)} + \frac{\overline{T}(\omega_i)}{T(\omega_i)} - \log \frac{\overline{T}(\omega_i)}{T(\omega_i)} - 2 \qquad (5)$$

Where:
n is the frequency points.
$T(\omega)$ is the transmissibility function from specific record of the baseline state condition.
$\overline{T}(\omega)$ is the identical transmissibility function for the same record, but from the suspected new condition.

On the one hand, for two spectra from same DOF for the same condition, COSH distance is entirely very close to zero. On the other hand, the higher the damage is in the beam, the larger the COSH measure will be, consequently, COSH distance will move away from zero.

The summation of the COSH distances over all the DOFs along the whole beam provides a global record to assess the differences between spectra from the intact reference condition and ambiguous state condition. This measure can be written as [16]:

$$\overline{C}(T, \overline{T}) = \frac{\sum_{j=1}^{m} C(T, \overline{T})}{m} \qquad (6)$$

Note that *m* represents the total number of DOFs, also with recorded averages for each particular FRF. Once more, in (6) is changed in this study to apply with the transmissibilities.

4. Numerical Verification

4.1. Model Description

As a verification test, this study adopts a freely supported model for a concrete beam of 2.0m length as a practical case study. Fig.1 shows the theoretical beam model used to generate the vibration data for different damage steps. The dimensions and the cross-section of the beam with the analysis details are shown in the Fig.1. The beam is modelled with 22 Bernoulli beam elements. The total mass of the beam is 57kg, which results in a density of the RC beam of ρ=2270kg/m^3. Additionally, the dynamic modulus of elasticity of the beam model is taken as E_c=27.5GPa.

For the intact reference state condition, the section dimensions of details shown in Fig.1 are employed in order to determine the gross moment of inertia. The effect of supporting chords was added by assuming an insignificant suspension stiffness of 1.0N/m to make sure stable condition problem. Through each damage status, a new stiffness matrix is generated based on the linear stiffness decrement given in Table 1.

4.2. Effect of Damage on Frequency Response Function FRF

One of the direct and simplest methods to detect the existence of the nonlinearity of a concrete structure, prevailing as cracks, relies on the raw FRF measurements. It was noted that a clear difference between the shapes of a drive point FRF (1, 1) measurement for a beam in different damage stages could provide a useful estimation of the degree of damage. The effect of damage development on the shape of drive point measurement for beam example is shown in Fig.2. As can be noted from this figure, there are clear shifts in resonance and anti-resonance to the left with the progress of damage. The shift in resonance becomes higher n the higher modes.

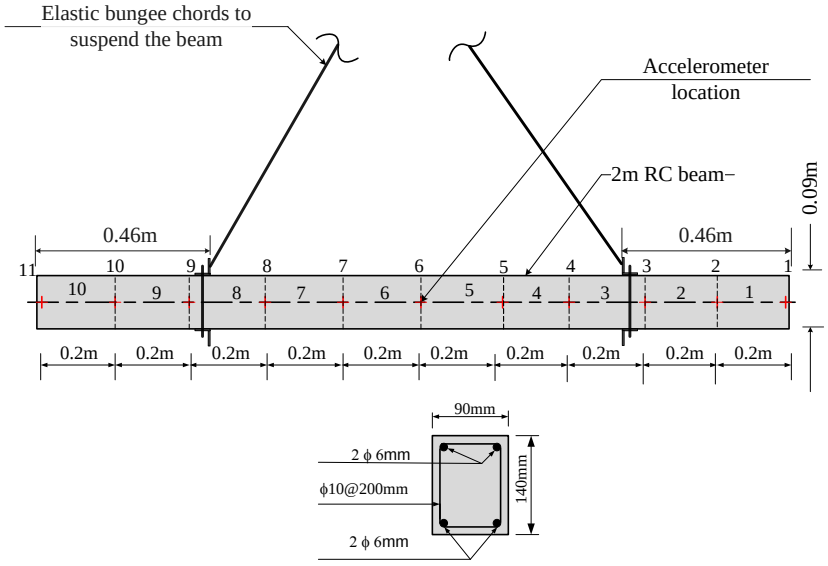

Figure 1. Arrangement of the verification beam test.

Table1. Induced damage conditions.

Damage status	Damage description
D0	healthy (intact) status
D1	50% reduction of stiffness in elements 1,2
D2	50% reduction of stiffness in elements 3,4
D3	10% reduction of stiffness in elements 5,6
D4	25% reduction of stiffness in elements 5,6
D5	50% reduction of stiffness in elements 5,6
D6	75% reduction of stiffness in elements 5,6

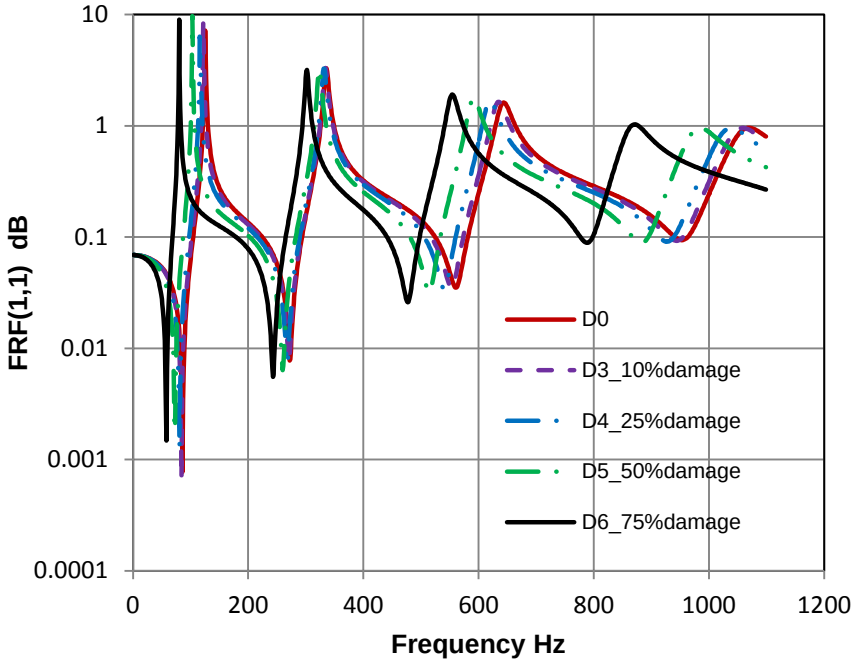

Figure 2. Frequency response functions FRF(1, 1) for different damage levels.

4.3. Effect of Damage on Transmissibility Functions

Transmissibility function as defined by (1) and (4) can be drawn between any two nodes' responses. Nonetheless, the results could be quite different. Therefore, to choose transmissibility is none an easy task that it influences the potential results significantly. In this study of the simple structure, all the transmissibilities can be plotted and analyzed afterward. Some prominent transmissibilities are calculated and plotted for different simulated defects. Fig.3 and Fig.4 show the transmissibility between the vertical displacements of node 6 (midspan) and node 1 (end point) TF(6,1) for various damage scenarios, given in Table 1. From Fig.3 and Fig.4, one can notice shifts in peaks of the resonance and anti-resonance frequencies, which can be utilized to detect the damage and its severity. The shift becomes higher for higher frequency and for severe damage. On the other hand, the damage is unnoticeable from the shift in the first frequency, for the small damage, and for damage between adjacent zones (D1 and D2), as shown in Fig.4.

Fig.5 shows the results of COSH distance for beam model of the verification example, which was estimated as given in (5) and (6). In this case, the distances were

obtained by comparing the transmissibility envelopes of all degrees of freedom (DOFs) and DOF 1, TF (all DOFs, 1), for each underlying damage case with the reference transmissibility spectra from the intact condition, as a reference data. The spectrum was collected from nodes 6 and 1 over the beam with the number of data points (n) considered in estimating the error between spectra from two different cases is (1100) points, cover frequency range of the transmissibility function of (1100Hz). The comparison reveals increases in the distance with the progress of deterioration. Most importantly, the damage level is reasonably quantified through COSH distance as shown in Fig.5. The higher the damage is introduced, the greater is the mean of COSH distance. The degree of damage is consistently arranged according to its significance.

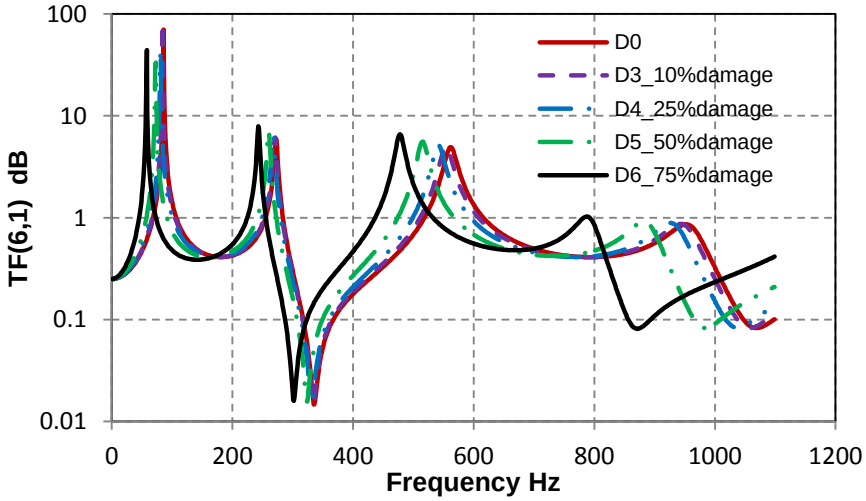

Figure 3. Transmissibility functions TF(6,1) for different damage levels elements 5,6

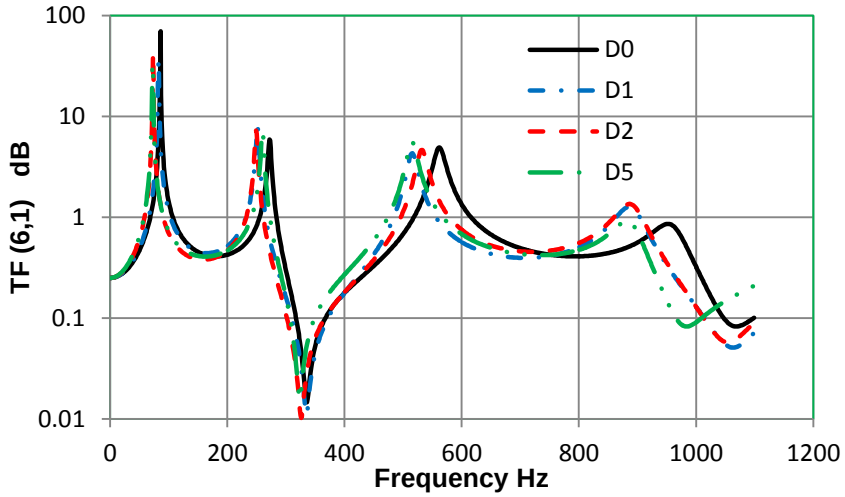

Figure 4. Transmissibility functions TF(6,1) for different damage levels

Once again, the COSH distance will be remarkably advantageous when it applied to the transmissibilities. The results of COSH distance for TF (all DOFs,1), as given in (5), and the mean of COSH distance for all the transmissibilities of the beam, as in (6) for the numerical beam model are shown in Fig.5.

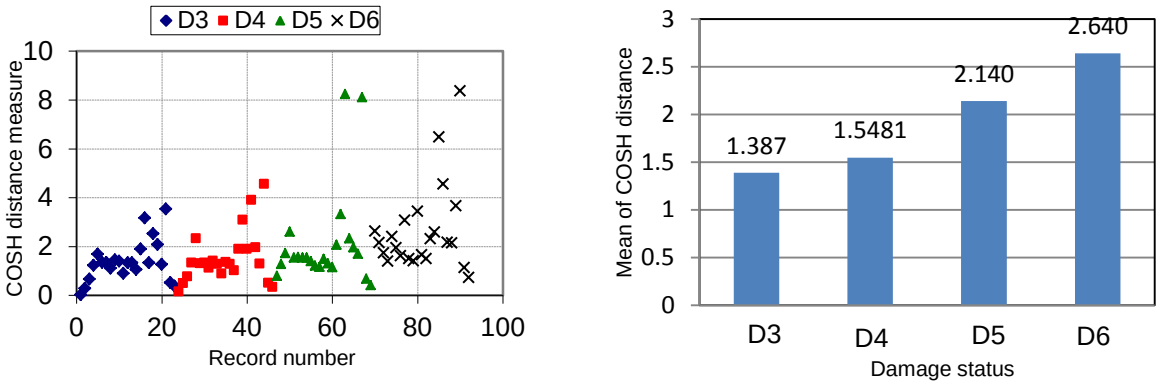

(a) (b)

Figure 5. (a) COSH distances over all DOFs with respect to the state condition, (b) Mean of COSH distance over all DOFs.

5. Experimental Verification

5.1 Test Beam

With the intention of examine the applicability of the proposed procedure on real life applications; a RC beam of the same properties given in Fig.1 was tested in freely support condition using EMA. In this test, the beam was suspended by two lightweight soft bungee cords attached at 0.23L (0.46m) from each end. Three accelerometers were fixed starting from the one end at distances of 0.2m apart, as given in Fig.6. After that, the three accelerometers were repositioned at three new positions so as to cover the entire length of the beam with a total of 11 measurement points. During the modal test, the beam was hit by a hammer and the accelerations were recorded normal to the direction of the elastic bungees. The acceleration response measurements were collected by using DeltaTron® 4514 accelerometers with sensitivities of 9.86mV/g and a frequency range is in the range 1–10 kHz. The dynamic force was generated by using the DeltaTron® type 8208 impact hammer with a sensitivity of 0.22mV/N containing frequency components up to 1100Hz. This study employed four-channel conditioning amplifier module NEXUS™ type 2690 whereby the input and output signals were simultaneously amplified and filtered, Fig.6.

In this modal testing, the first four modes were only covered with the current exciter. The force and response signals were captured for the entire beam sample on 11 positions using a four-channel data acquisition card with 4100 samples, taken at a rate of 8180 samples per second.

The experimental analyses of this beam case study of this research as well as the modal analyses results represent some outcomes of the author's PhD thesis [17].

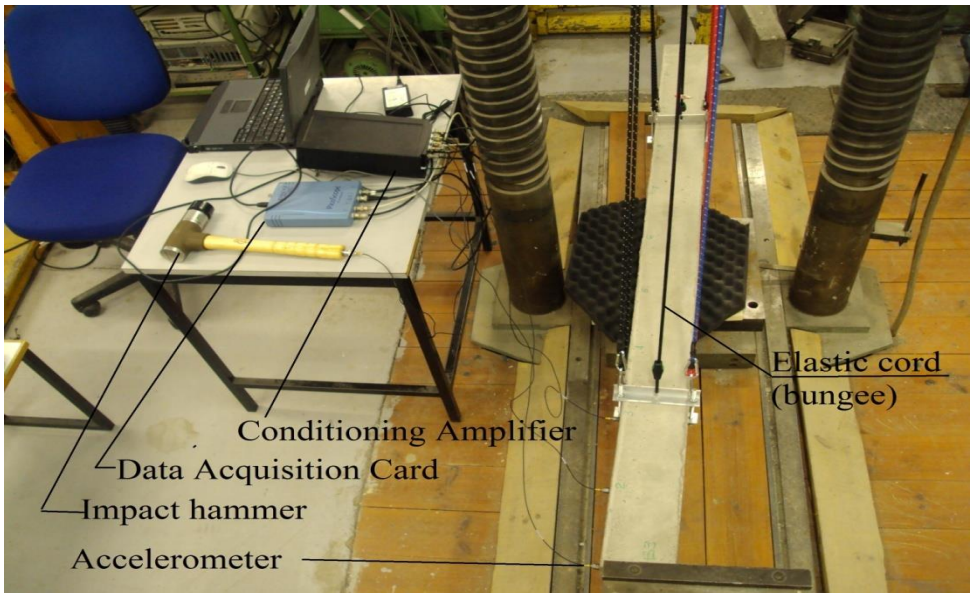

Figure 6. Experimental Modal Testing set-up of freely supported beam-photo.

5.2 Damage Set-Up

The experimental measurements were collected from 2.0m RC beam sample under seven consecutive loading conditions; explicitly intact, 3kN load, 6kN load, 10kN load, 13kN load, 15.5kN load and repaired beam. The test beam was subjected to two symmetrical point loads at 0.3m apart in order to create a four-point bending loading. The current testing display created a middle zone of evenly distributed defects due to the constant bending moment. The overall width distance between the supports of the universal machine was smaller than the length of the beam and equals 1.2m. Therefore, the span of the test beam was taken as 1.2m and an overhanging distance of 0.4m was left from each side. Then, the beam was subjected to five progressive load steps in the order given above in order to induce controlled levels of damage. At the end of each static load step, the beam was unloaded, and the simple supports were replaced by free-free supports to carry out EMA on a completely freely supported beam. At the final static loading step corresponding to15.5kN load when the beam became very fragile, the loading process was stopped, the cracking pattern thoroughly surveyed and the beam was tested then repaired. In the repair phase, the damaged area was strengthened by attaching a single layer of external carbon fiber reinforced polymer (CFRP).

5.3 Verification of Experimental Results

Fig.7 shows the FRF (1, 1), which is the response at end (1) of the beam when the excitation is at the same point (1), and its coherence function calculated from four group averages. As shown in Fig.7, a strong agreement was also achieved between the experimental FRF and its corresponding numerical FRF, after considering dynamic modulus of elasticity and proportional damping in the Euler-Bernoulli beam model.

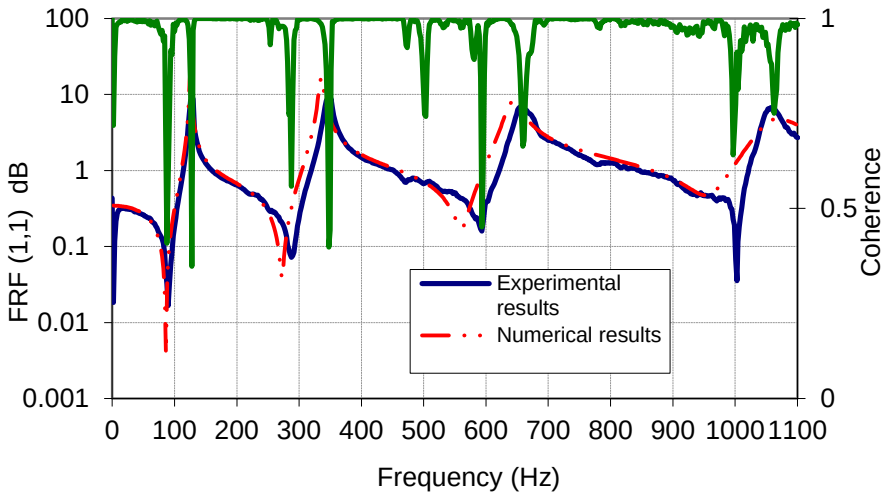

Figure 7. FRF and coherence functions from transducer 1 (right-hand end) when impact at 1 for intact beam.

5.4 .Transmissibility Comparison

In order to demonstrate the advantage of using the TF to detect damage, Fig.8 shows a comparison of TF(6, 1) under four different damage conditions; namely intact, 3kN, 15.5kN and repaired beam. From Fig.8 several vital observations can be mesmerized. Firstly, the transmissibility clearly managed to discriminate between different states of damage in the beam. The discrimination manifested as a clear shifts to the left for the four peaks with the progress of damage. Secondly, the transmissibility captured the four modes of vibration, but the resonance frequencies were not as those of FRF. Thirdly, in the cases of heavily loaded (15.5) as well as the repaired beam, the beam tended to has less sharp resonance peaks compared to the intact and lightly loaded beam (3kN), suggesting again development of higher damping with the escalating damage. In contrast, TF for the severely damaged beam showed multiple secondary peaks, which started to propagate, for higher frequencies. These local ripples appeared as an evident of nonlinear characteristics developed in the beams due to the effect of cracks.

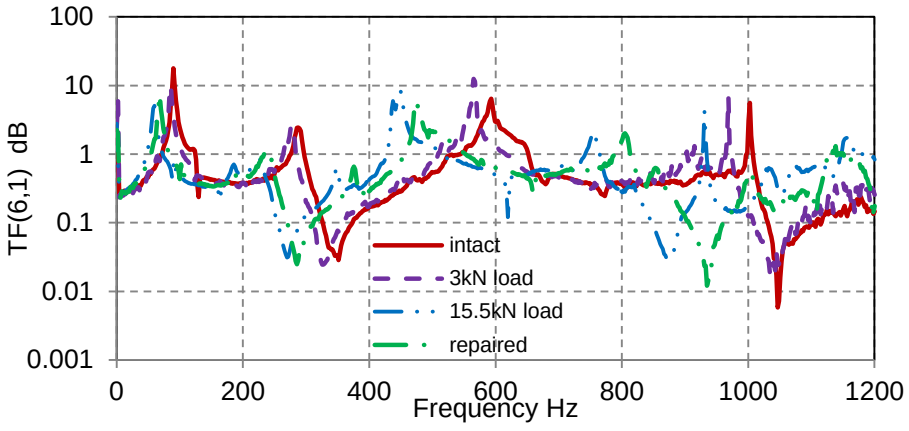

Figure 8: Experimental TF (6,1) for different damage conditions.

5.5 COSH Distance

The scale of change in COSH distance results for the FRFs of the beam is illustrated in Fig.9. The distances were computed using Equation 5, and by comparing (44) spectral envelopes for each damage case with (44) spectra from the intact reference case. For more details, the (44) spectra of particular case were recorded from 11 positions over the beam with (4) reiterations for each specific position. The number of data points (observations) considered in estimating the error between spectra of two different cases is (500) points that represent frequency range of a transfer function of (1000Hz). In this illustration, the comparison exposes clear variation in COSH distance; the variation could be as big as 7 times when the deterioration progresses from intact to severe. Nevertheless, it is factual that the increase in COSH distance is not consistent for all records of DOFs for a specific case because this depends upon the length of the envelope under consideration.

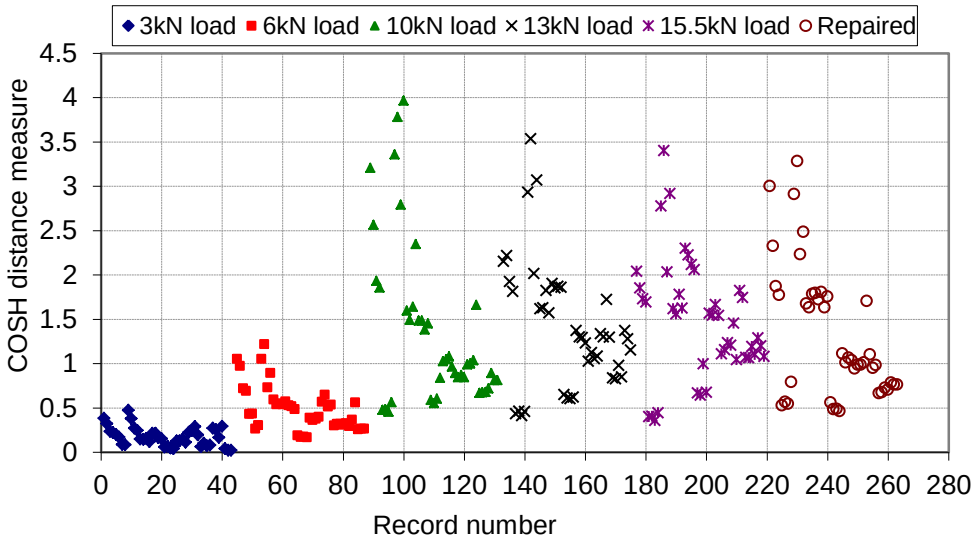

Figure 9. Variation of COSH discrete spectral distance with damage.

Also, the damage level can be discriminated through the mean of COSH distance over the DOFs, Equation 6. The results of mean COSH distance from experimental test beam are shown in Fig.10. The higher the damage is introduced, the greater is the mean of COSH distance. The degree of damage is consistently arranged according to its significance. Moreover, the effect of the repair done on the beam was noticeable by the mean value. The increase in the summation of all spectral distances with respect to the progressive damage was accurately and reasonably represented in Fig.10. This quantity can be utilized as a parameter to raise concern on abnormal behavior, after the value bypasses the threshold put for the normal case.

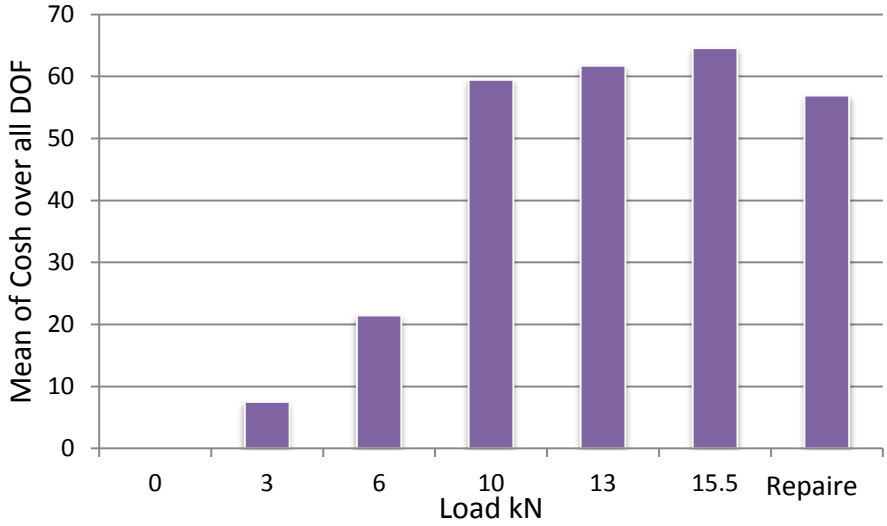

Figure 10. Means of COSH distances over all DOFs.

6. Conclusions

The study suggests using the transmissibility functions along with the COSH distance to detect, classify and discriminate between different levels of damage in RC beams.

The transmissibility function, as damage detection feature, has a significant advantage over the FRF as the first needs no effort to record the input excitation signatures. Feature sets from transmissibility data as a damage-sensitive parameter make SPR methods very fast and feasible to use in on-site or remote sensing SHM systems. The ability of the TF to detect low levels of damage in RC beams was verified using numerical simulation as well as real experimental data. The results showed credible ability in discrimination damage using the shift in frequency.

In the outlier detection context, the using of COSH distance and results of the mean COSH distance together with TF was proved successful in detecting the damage quantifiably, when a threshold value set to the intact reference datasets is crossed by likely damaged state. The extent of damage is consistently ordered by mean of COSH measurements according to its significance.

7. References

1. Hwang, H. and Kim, C. (2004).Damage Detection in Structures Using a Few Frequency Response Measurements, Journal of Sound and Vibration, Vol.270, issue 1: pp 1-14.
2. Carden, P. and Brownjohn, J. M.W. (2008).ARMA modelled time-series classification for structural health monitoring of civil infrastructure, Mechanical Systems and Signal Processing 22, pp. 295–314.
3. Zhou Yun-Lai, Figueiredo E., Maia N., and Perera R. (2015).Damage Detection and Quantification Using Transmissibility Coherence Analysis, Shock and Vibration, Volume 2015, Article ID 290714.

4. Wenzel H. (2009).Health Monitoring of Bridges, John Wiley & Sons Ltd, West Sussex, United Kingdom.
5. Farrar C., Doebling S. and Nix D. (2001).Vibration-Based Structural Damage Identification. Philosophy Transactions Royal Society, Vol. 359: pp 131-149.
6. Sohn, H., Farrar, C., Hunter, H. and Worden, K. (2001).Applying the LANL Statistical Pattern Recognition Paradigm for Structural Health Monitoring to Data from a Surface-Effect Fast Patrol Boat. Technical Report LA-13761-MS, Los Alamos National Laboratory, Los Alamos, New Mexico.
7. Brownjohn, James M.W, De Stefano Alessandro, Xu You-Lin, Wenzel Helmut, Aktan, A. Emin. (2011).Vibration-based monitoring of civil infrastructure: challenges and successes, Journal of Civil Structural Health Monitoring, DOI 10.1007/s13349-011-0009-5.
8. Worden, K. (1997).Structural Fault Detection Using a Novelty Measure, Journal of Sound and Vibration, Vol. 201, Issue 1: pp 85-101.
9. Worden, K., Manson, G. and Fieller, NRJ. (2000).Damage Detection Using Outlier Analysis, Journal of Sound and Vibration, Vol. 229, Issue 3: pp 647-667.
10. Balageas, D., Fritzen, CP. and Gemes, A. (2006).Structural Health Monitoring. ISTE.
11. Worden, K., Manson, G. and Allman, D. (2003).Experimental Validation of A Structural Health Monitoring Methodology: Part I. Novelty Detection on A Laboratory Structure, Journal of Sound and Vibration, 259(2), pp. 323–343.
12. Carrella, A. Ewins, J. and Harper, L. (2011).Using Transmissibility measurements for Nonlinear Identification, Proceedings of the 29th IMAC, A conference on structural dynamics, Modal Analysis Topics, Volume 3, Jacksonville, Florida, January 31 - February 3, 2011.
13. DTA. (1993).Handbook on Guidelines to Best Practice, Volume 3, Modal Testing. The Dynamic Testing Agency, UK.
14. Ewins, D. (2000).Modal Testing: Theory, Practice and Application, Research Studies Press Ltd. Baldock, Hertfordshire, England.
15. McConnell, K. and Varoto P. (2008). Vibration Testing: Theory and Practice, John Wiley & Sons, Inc., USA.
16. Trendafilova, I. (2011).A Method for Vibration-Based Structural Interrogation and Health Monitoring Based on Signal Cross-Correlation, 9th International Conference on Damage Assessment of Structures (DAMAS 2011), Journal of Physics: Conference Series, Vol. 305.
17. Al-Ghalib, A.A. (2013).Damage and Repair Identification in RC Beams Modelled with Various Damage Scenarios Using Vibration Data, PhD. Thesis, Nottingham Trent University, Nottingham, UK.